Interaction of the Hydrogenase Accessory Protein HypC with HycE, the Large Subunit of *Escherichia coli* Hydrogenase 3 during Enzyme Maturation†

Nikola Drapal and August Böck*

Lehrstuhl für Mikrobiologie der Universität München, Maria-Ward-Strasse 1a, 80638 München, Germany

Received August 13, 1997

ABSTRACT: Maturation of the large subunit of *E. coli* hydrogenase 3, HycE, requires the action of seven accessory proteins. The HycI protease catalyses a C-terminal proteolytic cleavage of the large subunit, which was shown to result in a dramatic change in migration behavior of HycE in nondenaturing PAGE. HypA, HypB, HypC, HypD, HypE, and HypF are required for metallocenter assembly. A polyacrylamide gel system under nondenaturing conditions was used for the investigation of any protein−protein interactions between HycE and the Hyp proteins. It revealed the existence of a complex between the precursor of HycE (pre-HycE) with one of the accessory proteins, namely HypC. HypC migrates in at least three different forms in nondenaturing PAGE, the appearance of one of which (form 1) is strictly dependent on the presence of unprocessed HycE in the extract. Overexpression of either *hypC* or *hycE* from a plasmid leads to an increased formation of this HypC-form 1. In two-dimensional polyacrylamide gel electrophoresis with nondenaturing PAGE as the first and SDS-PAGE as the second dimension, this HypC form comigrates with part of the pre-HycE protein. This comigration was also observed in anion exchange chromatography. To analyze the pre-HycE-HypC complex in more detail, HypC was overproduced and purified. The purified protein was able to bind to pre-HycE in vitro. These results and also the finding that the processed form of HycE is not associated with HypC suggest that HypC binds to pre-HycE to keep it in a conformation accessible for metal incorporation.

Hydrogenase 3 of *E. coli* is a structural component of the formate hydrogen−lyase complex (*1*). Under fermentative conditions, this enzyme catalyzes the disproportion of the acidic fermentation product formate into H_2 and CO_2. The electrons produced by formate dehydrogenase H during formate oxidation are transferred to hydrogenase 3, a H_2-evolving enzyme.

Hydrogenase 3 belongs to the [NiFe] type of hydrogenases, which were recently shown to contain a rather unusual and complex active site located on the large subunit of the enzyme. In the case of the *Desulfovibrio gigas* enzyme, Ni is coordinated by four cysteine residues, which are strictly conserved also among [NiFe] hydrogenases from other organisms. Two of the cysteine-derived thiolates form a bridge to a second metal, Fe, which is additionally coordinated by three nonprotein derived ligands (*2*). Recently, these ligands were identified as one CO and two CN molecules (*3*).

The large subunit of [NiFe] hydrogenases is synthesized in a precursor form that is devoid of the active site metallocenter. In a complex maturation process, which requires the function of a number of accessory proteins (reviewed in ref *4*), the metallocenter is assembled posttranslationally. The posttranslational maturation of *E. coli* hydrogenase 3 has been investigated in some detail. In an in vitro system, Ni-incorporation into the large subunit, C-terminal processing catalyzed by a specific protease, HycI, and the generation of hydrogenase activity were demonstrated (*5*−*7*). In vitro Ni-dependent processing of the hydrogenase large subunit has also been demonstrated in *Azotobacter vinelandii* (*8*).

A role in metallocenter assembly was assigned to the proteins HypA, HypB, HypC, HypD, HypE, and HypF, since a deletion in each of the corresponding genes (*hyp*) leads to the accumulation of the Ni-free precursor form of the large subunit, pre-HycE (*9*−*11*). Indeed, in vitro Ni-incorporation into pre-HycE was dependent on the presence of the Hyp proteins, although it could not be excluded that Hyp functions might concern maturation steps preceding Ni-incorporation (*7*). Until now a specific function could not be assigned to any of the Hyp proteins.

HypA, besides being required for Ni-incorporation, was shown to modulate hydrogenase 2 activity in *E. coli* in an unknown manner (*9*). A deletion in the *hypB* gene can be complemented by high Ni concentrations in the growth medium (*12*). Therefore, a role in Ni-donation was proposed for it. HypB from *E. coli* was shown to exhibit GTPase activity (*10*), which is essential for Ni-incorporation into pre-HycE (*13*). *Bradyrhizobium japonicum* HypB is supposed to play a role in both Ni-storage and Ni-dependent transcriptional regulation of hydrogenase gene expression (*14*).

To be able to define a more specific function of the Hyp proteins, we decided to investigate putative interactions between these accessory proteins and the large subunit of hydrogenase 3, HycE. A nondenaturing polyacrylamide gel system was established to this end, that allows immunological detection of protein−protein complexes.

† This work was supported by grants from the Deutsche Forschungsgemeinschaft (Bo 305/22-1) and the Fonds der Chemischen Industrie.

S0006-2960(97)02007-2 CCC: $15.00
Published on Web 02/11/1998

Table 1: *E. coli* Strains and Plasmids Used in This Study

strain/plasmid	genotype	reference
JM109	*recA1*, *endA1*, *gyrA96*, *thi*, *hsdR17*, *supE44*, *relA1*, λ^-, Δ(*lac*−*pro*AB)	30
MC4100	F$^-$, *araD*139, Δ(*argF*-lac)−*U169*,*pts*F25, *rel*A1, *flb*B5301, *rps*L150, λ^-	31
HD705	MC4100, Δ*hycE*	32
EDC32	MC4100, 96-bp deletion in *hycE* (from nucleotides 1,611 to 1,707)	26
HD709	MC4100, Δ*hycI*	26
NCI900	HD709, *nikA*::Mud*I*	7
HYD720	MC4100, Δ*nikA-E*	33
NST22	MC4100, *hycE-Strep-tagII*, *nikA*::Mud*I*	23
SMP101	MC4100, *hypA* (ATG→TAA)	9
DHP-B	MC4100, Δ*hypB*	9
DHP-C	MC4100, Δ*hypC*	9
DHP-D	MC4100, Δ*hypD*	9
DHP-E	MC4100, Δ*hypE*	9
DHP-F	MC4100, Δ*hypF*	11
BL21(DE3)	*E.coli B*; F$^-$, *hsdS*, gal1, DE3	19
pACE1	Cm^R, 2506bp fragment (*hycD′*, *hycE*, *hycF′*) in pACYC184	Mintz-Weber, & Böck, unpublished
pJA1021	Cm^R, 350bp fragment (*hyp*C) in pACYC184	9
pUC19	Ap^R, *lac′IPOZ′*	30
pCFus-7	Ap^R, 350bp *Bam*HI fragment (*hyp*C) from pJA2621 in pT7−7	unpublished
pJA2621	Ap^R, 350bp fragment (*hyp*C) via *Bam*HI linkers in pT7−6	34
pC1-8	Ap^R, 273bp fragment (*hyp*C) in pUC19 (*Nde*I, *Eco*RI)	this work
pT7-7	Ap^R, T7Φ10	18
pTC-9	Ap^R, 273bp fragment (*hyp*C) in pT7−7 (*Nde*I, *Eco*RI)	this work

EXPERIMENTAL PROCEDURES

Bacterial strains, Growth Conditions, and Extract Preparation. The *E. coli* strains used in this study are listed in Table 1. Bacteria were grown anaerobically in TGYEP medium (*15*) containing 30 mM sodium formate. For cultivation of strain HYD720 and NST22, 50 μM EDTA[1] was added to the medium to minimize unspecific Ni-uptake by the Mg-uptake system (*16*) and thus reduce premature processing of pre-HycE. When required, antibiotics were added at the following final concentrations: ampicillin 100 μg/mL and chloramphenicol 30 μg/mL. At an OD_{600} of 1, cells were harvested and washed once with buffer A (50 mM potassium phosphate pH 7.5, 1 mM DTT, 1 mM benzamidine).

S-100 extracts used for nondenaturing PAGE were prepared as follows: anaerobically grown cells from a 250 mL culture were resuspended in 1 mL of 50 mM potassium phosphate buffer containing 1 mM DTT. After addition of 20 μg/mL DNaseI and PMSF each, cells were disrupted by passage through a French press cell at 12000 psi. After removing cell debris by centrifugation at 10000*g* for 20 min, the supernatant was clarified from membranes by centrifugation at 100000*g* for 2 h. S-100 extracts (protein concentration around 15 mg/mL) were either used immediately or shock-frozen in liquid nitrogen in small aliquots and stored at −70 °C.

Plasmid Construction. Strain JM109 was used as a host in plasmid constructions. For construction of pTC-9 the *hypC* gene was amplified by PCR. To generate appropriate restriction sites (*Nde*I and *Eco*RI), the degenerate oligonucleotides HypC-1b (5′-GGAATTCCATATGTGCATAG-GCGTTCCCGGCCAG-3′) and HypC-2 (5′-GGAATTCT-TATTTTTCCTCGCCATAC-3′) were used. After restriction with *Nde*I and *Eco*RI the PCR product was cloned into pUC19 to generate plasmid pC1-8. Dye Terminator Cycle-Sequencing confirmed the correct nucleotide sequence of the PCR product, which was then transferred into plasmid pT7-7 to yield plasmid pTC-9.

Polyacrylamide Gel Electrophoresis and Immunoblotting Analysis. SDS-PAGE was performed according to (*17*). For PAGE under nondenaturing conditions the following modifications were made: S-100 extracts were used only. SDS was omitted from buffers. As sample buffer 60 mM Tris-HCl pH 6.8, 10% glycerol, and 0.01% bromophenol blue was used and samples were applied to the gel without prior heating. The voltage did not exceed 100 V during electrophoresis.

For 2D-gel electrophoresis, the S-100 extract was separated first by PAGE in the absence of SDS (12.5%, first dimension), and the appropriate lane was cut out from the gel. The strip was soaked in 3 x cracking buffer (*18*) for 10 min and subsequently applied horizontally to a 15% SDS-polyacrylamide gel (second dimension).

For immunoblotting analysis, proteins were transferred onto nitrocellulose membranes, whereby methanol was omitted from the blotting buffer after nondenaturing PAGE. Anti-HycE antibodies were used at a dilution of 1:1500. For detection of HypC, an antiserum against a HypC-fusion protein with an N-terminal extension of 22 amino acids was used at a dilution of 1:500. Overproduction of this fusion protein was performed in strain BL21(DE3) and directed from plasmid pCFus-7. For antibody detection, the Protein A-Horseradish Peroxidase Conjugate (Bio-Rad) and the Chemiluminescence Blotting Substrate from Boehringer Mannheim were used.

Purification of Native HypC. For overproduction of native HypC, plasmid pTC-9 was transformed into strain BL21-(DE3) (*19*). Cells were grown aerobically in LB-medium (*20*) containing 150 μg/mL ampicillin. At an OD_{600} of 1 *hypC* expression was induced by addition of 0.5 mM IPTG. After additional 3 h of incubation, cells were harvested and washed once with buffer A.

[1] Abbreviations: EDTA, ethylenediaminetetraacetic acid; DTT, dithiothreitol; PMSF, phenylmethylsulfonyl fluoride; psi, pounds per square inch; PAGE, polyacrylamide gel electrophoresis; PCR, polymerase chain reaction; IPTG, isopropyl-β-thiogalactopyranoside; SDS, sodium dodecyl sulfate.

All following steps were performed at 4 °C. A 3 g amount of cells (wet weight) was resuspended in 3 mL of buffer B (50 mM potassium phosphate pH 7.4, 1 mM DTT, 1 mM EDTA). After addition of 20 μg/mL DNaseI and PMSF, a crude extract was prepared by passage through a French press cell at 16000 psi. Following two centrifugation steps (30 min at 10000*g* and 2 h at 100000*g*), the supernatant was diluted to a protein concentration (*21*) of 10 mg/mL with buffer B. Solid ammonium sulfate was added up to 50% saturation, and the resulting pellet was resuspended in 2 mL of buffer B and dialyzed against the same buffer for 12 h. After removing insoluble material by centrifugation, the sample was applied to a 1 mL Mono-Q column (Pharmacia) equilibrated with buffer B. The flow rate was 30 mL/h. Using a 30 mL linear gradient ranging from 0 to 500 mM KCl, HypC eluted from 100 to 270 mM KCl. The fractions containing highly enriched HypC were pooled and concentrated in Centricon-10 concentrators (Amicon) to a volume of 1 mL which was next applied to a Superdex 75 gel filtration column (Pharmacia) equilibrated in buffer B containing 100 mM KCl. The flow rate was 60 mL/h. Fractions containing apparently pure HypC were pooled and dialyzed against buffer B containing 50% glycerol. About 2.8 mg of HypC was obtained.

For overproduction of HypC which should be used for atomic absorption spectroscopy (AAS), the growth medium was supplemented with 100 μM of $NiCl_2$ and $Fe(II)SO_4$ each, and EDTA was omitted from buffers during the purification.

Purification of Pre-HycE. Pre-HycE was purified using *Strep-tag II* affinity technology (*22*). Strain NST22 was used for that purpose, in which the wild-type *hycE* gene was replaced by a construct carrying a *Strep-tag II*-peptide sequence (NWSHPQFEK) fused N-terminally to the *hycE* gene (*23*). Furthermore, as a consequence of a genetic lesion in the Ni-specific uptake system, HycE accumulates as the Ni-free precursor form in this strain (*Strep-tag II* pre-HycE (*nik*)). Growth of the cells, extract preparation, ammonium sulfate precipitation, and affinity purification of *Strep-tag II* pre-HycE (*nik*) on a Streptactin−Sepharose column were performed exactely as described in ref *23*. After affinity chromatography, HycE containing fractions were pooled and dialyzed against 2 L of buffer C (50 mM potassium phosphate buffer pH 7.5, 1 mM EDTA, 0.1 mM DTT) for 16 h. After removing insoluble material by centrifugation, the sample was applied to a 1 mL Mono-Q column equilibrated with buffer C at a flow rate of 30 mL/h. Proteins were eluted with a 20 mL of linear gradient ranging from 0 to 500 mM NaCl. Next, the fractions were tested for HycE and HypC immunologically so that *Strep-tag II* pre-HycE (*nik*) containing fractions could be separated from fractions "contaminated" with processed HycE species or HypC. *Strep-tag II* pre-HycE (*nik*) was brought to a final concentration of 0.17 mg/mL using Centricon-30 concentrators.

In Vitro Processing and Complex Formation. In vitro processing was performed as described recently (*7*) except that S-100 extracts were used. When subjected to PAGE under nondenaturing conditions, the SDS-free sample buffer was added after incubation.

In vitro complex formation between pre-HycE and HypC was investigated either in S-100 extracts or with purified components. Complex formation in extracts was performed according to the following protocol: 340 ng of purified HypC was added to 9 μL of S-100 extract of strain HD705 or DHP-C grown anaerobically. After 30 min incubation at 30 °C, SDS-free sample buffer was added, the sample subjected to nondenaturing PAGE (12.5%), and HypC was detected by immunoblotting analysis. For the investigation of complex formation with purified components, 0.85 μg of *Strep-tag II* pre-HycE (*nik*) was incubated with 0.85 μg of HypC for 30 min at 30 °C. After 10% nondenaturing PAGE, HypC was detected immunologically.

Coelution of Pre-HycE and HypC. A 500 μL amount of S-100 extract of strain HD709 or DHP-C was applied to a 1 mL Mono-Q column equilibrated in buffer C. The flow rate was 30 mL/h. Proteins were eluted from the column with a 20 mL linear gradient ranging from 0 to 500 mM NaCl. Pre-HycE-HypC complex containing fractions were detected by nondenaturing PAGE and immunological analysis with anti-HypC antiserum. The presence of HycE in these fractions was determined by SDS-PAGE and immunological detection with anti-HycE antibodies.

RESULTS

Change of Migration Behavior of HycE after in Vitro Processing. To test the suitability of the chosen nondenaturing polyacrylamide gel system, an in vitro processing reaction was performed using strain NCI900. In this strain HycE accumulates in a nickel-free precursor form as a consequence of genetic lesions, one in the gene encoding the hydrogenase 3 specific protease (*hycI*) and the other in the Ni-specific uptake system (*nik*) (*7*, *24*). Addition of purified HycI protease and $NiCl_2$ to an extract of this strain allows Ni-incorporation into the active site of pre-HycE and C-terminal processing to take place (*7*). The removal of a 3.85 kD peptide (*5*) and the expected conformational change internalizing the metal center into the interior of the protein (*2*) should lead to a change in the migration behavior of HycE.

An S-100 extract was prepared from anaerobically grown NCI900 cells. After addition of either 400 μM $NiCl_2$ or purified HycI (0.5% of total protein) or of both components together and incubation at 30 °C for 60 min, the samples were applied to 10% nondenaturing PAGE (Figure 1, top) and to a 10% SDS-PAGE (Figure 1, bottom). Most of the HycE antigen in NCI900 migrates slowly in multiple bands (lane 2, top) which consist of the precursor form of HycE (lane 2, bottom). Neither the addition of $NiCl_2$ (lane 3) nor of HycI protease (lane 4) alone results in processing (bottom) or in any change of the migration behavior (top). Only upon addition of both components (lane 5) processing takes place (lane 5, bottom) to about 30% as determined by laser densitometry. Processing is accompanied by a dramatic change in migration behavior and the generation of a new HycE form (lane 5, top). About 50% of the HycE antigen migrates in this form, which corresponds to the predominant HycE form found in the wild-type (MC4100, lane 1 and 6, top).

Migration Behavior of HypC upon Nondenaturing Polyacrylamide Gel Electrophoresis. To investigate possible interactions between HycE and any of the accessory Hyp proteins, S-100 extracts from strains with mutations in genes required for hydrogenase activity were separated by nondenaturing PAGE, and Western blot experiments were

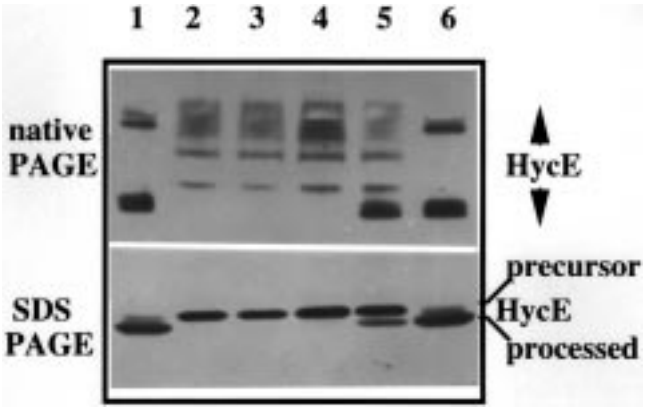

FIGURE 1: Change of migration behavior of HycE after processing in vitro. Chemoluminogram of extracts of *E. coli* MC4100 (wt; lanes 1 and 6) and NCI900 (Δ*hycI*, *nikA*⁻; lanes 2−5). Processing reactions were performed with strain NCI900 without addition of $NiCl_2$ and HycI (lane 2), in the presence of 400 μM $NiCl_2$ (lane 3), in the presence of purified HycI protease (0,5% of total protein; lane 4), or in the presence of both 400 μM $NiCl_2$ and HycI protease (lane 5). Samples were applied to nondenaturing PAGE (top) or SDS-PAGE (bottom). HycE was detected immunologically with α-HycE antibodies.

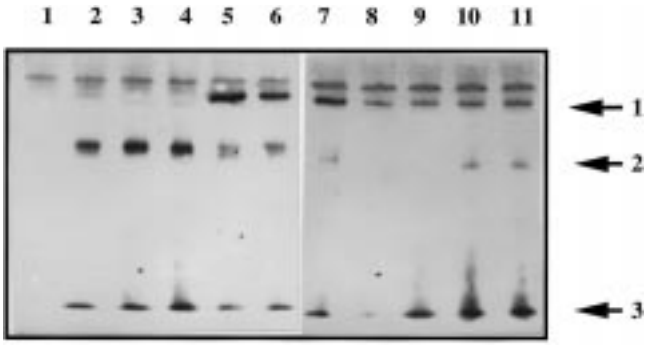

FIGURE 2: HypC-forms in extracts from strains with mutations in genes required for hydrogenase activity. Chemoluminogram of extracts from strains DHP-C (Δ*hypC*; lane 1), MC4100 (wt; lane 2), HD705 (Δ*hycE*; lane 3), EDC32 (Δ*hycE* C-terminus; lane 4), HD709 (Δ*hycI*; lane 5), HYD720 (*nik*⁻; lane 6), SMP101 (*hypA*⁻; lane 7), DHP-B (Δ*hypB*; lane 8), DHP-D (Δ*hypD*; lane 9), DHP-E (Δ*hypE*; lane 10) and DHP-F (Δ*hypF*; lane 11). HypC-forms were detected with α-HypC antiserum and are marked with arrows.

performed employing antisera directed against HypB, HypC, HypD, HypE, and HypF.

The migration behavior of HypB, HypD, HypE, and HypF did not vary in any of the mutants tested (data not shown). The migration behavior of HypC, on the other hand, was different in various mutants. Up to three different HypC-forms could be detected (Figure 2). HypC-form 2 is lacking in strains DHP-B (lane 8) and DHP-D (lane 9) whereas HypC-form 3 is present in all mutants tested. Most interestingly, HypC-form 1 is present in all strains except those devoid of an intact *hycE* gene (HD705 and EDC32, lanes 3 and 4). In the wild-type strain (MC4100, lane 2), only trace amounts of form 1 are detectable. These results suggest that the HypC-form 1 could be due to an interaction of HypC with the precursor form of HycE.

To test whether the presence and the amount of HypC-form 1 could be influenced by overproduction of one of the potential partners, plasmids carrying the *hypC* gene (pJA1021) or the *hycE* gene (pACE1) were transformed into MC4100 (wt) and HD705 (Δ*hycE*), respectively. After growing the

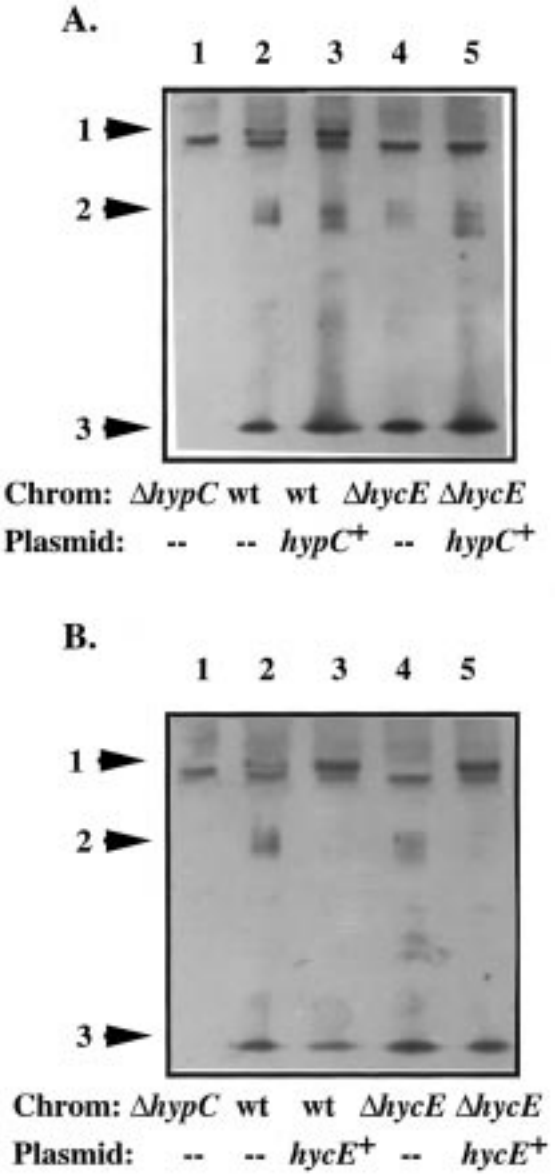

FIGURE 3: Effect of overproduction of HypC or HycE from a plasmid on the quantity of HypC-form 1. Chemoluminogram. A: Overproduction of HypC: DHP-C (lane 1), MC4100 (lane 2), MC4100 pJA1021 (lane 3), HD705 (lane 4), HD705 pJA1021 (lane 5). B: Overproduction of HycE: DHP-C (lane 1), MC4100 (lane 2), MC4100 pACE1 (lane 3), HD705 (lane 4), HD705 pACE1 (lane 5). After nondenaturing PAGE, HypC-forms were detected immunologically using α-HypC antiserum.

cells anaerobically, S-100 extracts were prepared, the proteins were separated by nondenaturing PAGE, and the migration behavior of HypC was detected immunologically (Figure 3). Overproduction of HypC in a wild-type background leads to an increase in the amount of HypC-form 1 (Figure 3A, lane 3), whereas this form 1 cannot be generated by overproduction of HypC in a Δ*hycE* background (Figure 3A, lane 5). Interestingly, overproduction of HycE leads to a drastic change of HypC migration. In the wild-type as well as in the Δ*hycE* strain, *hycE* expression from a plasmid leads to an increase in the amount of HypC-form 1 and the disappearance of HypC-form 2 (Figure 3B, lanes 3 and 5). Therefore, overproduction of each one of the interacting partners leads to an increase in the amount of the pre-HycE-HypC complex.

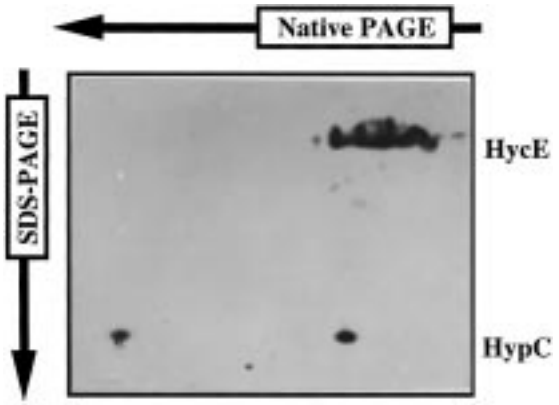

FIGURE 4: Two-dimensional gel electrophoresis and immunological detection of HycE and HypC. Chemoluminogram of a HD709 extract subjected to nondenaturing PAGE (first dimension) and subsequently to SDS-PAGE (second dimension). After transfer of the proteins to nitrocellulose, the membrane was incubated with α-HycE antibodies and α-HypC antiserum.

Comigration of Pre-HycE with HypC-form 1. So far, the existence of a pre-HycE-HypC complex has only been inferred from the influence of pre-HycE in the extract on the occurrence of HypC-form 1. For a more direct proof, comigration experiments were performed.

Due to the undefined migration behavior of pre-HycE in nondenaturing PAGE (Figure 1, lanes 2−4) and the fact that this migration behavior does not change in a Δ*hypC* mutant, DHP-C (data not shown), it was impossible to perform comigration experiments in a one-dimensional gel system. Therefore, a two-dimensional gel system with nondenaturing PAGE in the first and SDS-PAGE in the second dimension was established to demonstrate the presence of pre-HycE at the same migration position in nondenaturing PAGE as HypC-form 1. A HD709 S-100 extract was used for this experiment, since the HypC-form 1 is most abundant in this strain. After transferring the proteins onto nitrocellulose, HycE and HypC were detected immunologically (Figure 4). As already shown in Figure 1, the HycE precursor migrates as a smear under nondenaturing conditions. HypC in contrast migrates in two distinct forms. One of them corresponds to the HypC-form 1 and is clearly associated with part of the pre-HycE antigen, while the other form corresponds to the fast migrating HypC-form 3 observed in earlier experiments. For reasons not known, the third HypC form (form 2) could not be detected in this case.

Comigration of pre-HycE and HypC can also be observed during anion exchange chromatography. S-100 extracts of strain HD709 (Δ*hycI*, Figure 5A) or DHP-C (Δ*hypC*, Figure 5B) were applied to a Mono-Q column, proteins were eluted with a linear gradient ranging from 0 to 500 mM NaCl, and fractions were tested for HypC and HycE immunologically (Figure 5). HypC-form 1 is retarded by the column and elutes in the fractions 8 to 11 (Figure 5A, top). In the same fractions part of the HycE precursor can be found (Figure 5A, bottom). However, the occurrence of this form of pre-HycE in these fractions depends on the presence of HypC in the extract, as this pre-HycE form cannot be detected in fractions 8−11 when the same experiment is performed with a Δ*hypC* strain (Figure 5B). HypC-form 3 binds to the Mono-Q column and elutes between 90 and 350 mM NaCl (data not shown). HypC-form 2 could not be detected in the fractions (data not shown).

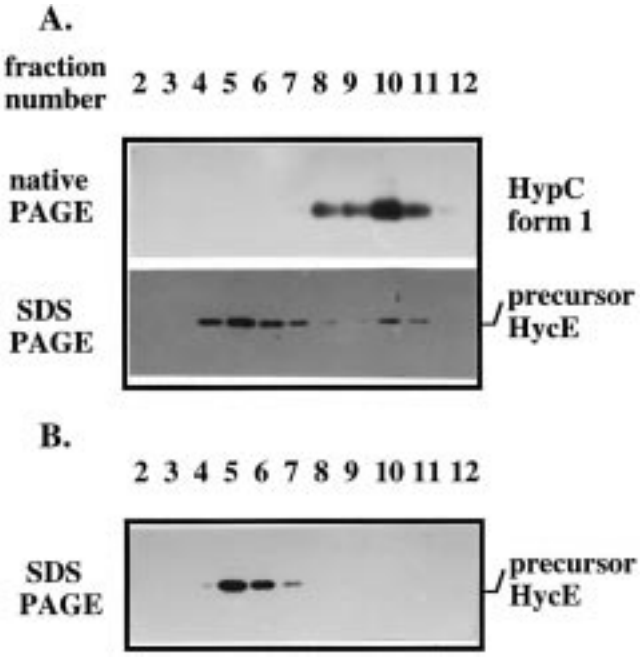

FIGURE 5: Coelution of pre-HycE and HypC from a Mono-Q column: Chemoluminograms of extracts from strains HD709 (A) and DHP-C (B). After application of extracts to a Mono-Q column, fractions were analyzed for HypC-form 1 (A, upper pannel) or HycE protein (A, lower pannel and B) by immunoblotting analysis.

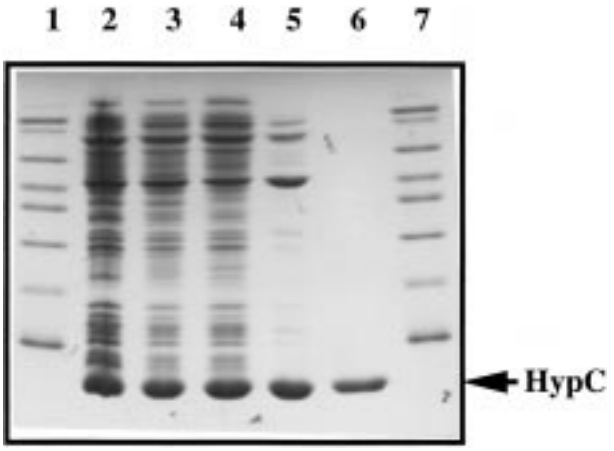

FIGURE 6: Purification of native HypC. Samples were separated by 15% SDS-PAGE and stained with Coomassie blue: marker proteins (lane 1 and 7; 97 kD, 85 kD, 55 kD, 39 kD, 33 kD, 27 kD, 19 kD, 14 kD), S-10 extract (lane 2), S-100 extract (lane 3), desalted pellet of 0 to 50% ammonium sulfate precipitation (lane 4), HypC containing fractions after anion exchange chromatography (lane 5), and purified HypC after gel filtration (lane 6).

Purification of Native HypC. To analyze the pre-HycE-HypC complex in more detail, native HypC was purified. To get maximal overproduction, *hypC* was expressed from vector pTC-9, a pT7−7 derivative, in strain BL21(DE3). It yielded soluble protein (Figure 6, lanes 2 and 3). After ammonium sulfate precipitation, HypC was purified by two chromatographic steps. First, the desalted pellet (Figure 6, lane 4) was subjected to anion exchange chromatography (Figure 6, lane 5). Gel filtration chromatography as a second step yielded apparently homogeneous HypC protein (Figure 6, lane 6) which eluted at the position of an 18 kD protein. Therefore, under these conditions HypC seems to form a dimer.

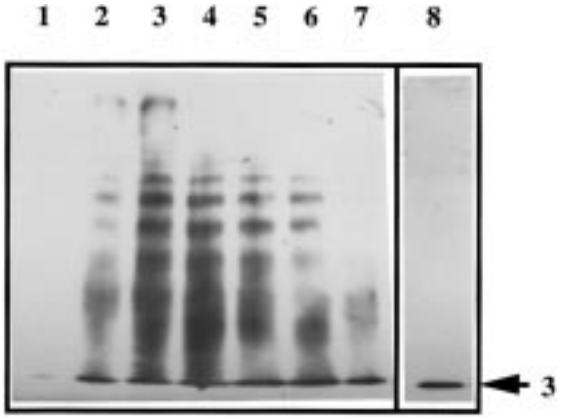

FIGURE 7: Migration behavior of purified HypC in nondenaturing PAGE. Chemoluminogram. Fractions 28−34 (lanes 1−7) after gel filtration were subjected to 15% nondenaturing PAGE and HypC was detected by immunoblotting analysis using α-HypC antiserum. Lane 8 shows the migration behavior of purified HypC after filtration through a 50 kD size-exclusion membrane. HypC-form 3 is marked by an arrow.

An UV/visible spectrum of the purified protein did not indicate the presence of any cofactor (data not shown). Purified HypC also was tested for Ni- or Fe-binding by atomic absorption spectroscopy. Less than 0.04 mol of Fe and Ni each was found per mole of HypC.

Migration Behavior of Purified HypC in Nondenaturing PAGE. To find out if one of the three HypC-forms found in nondenaturing PAGE corresponds to free, dimeric HypC, the Superdex 75 fractions containing apparently pure HypC (Figure 6, lane 6) were subjected to 15% nondenaturing PAGE, and HypC was detected by immunoblotting analysis. Surprisingly, HypC migrated not in one single form but as a ladder of forms, which could consist of HypC oligomers (Figure 7, lanes 1 to 7). When purified HypC was submitted to filtration through a membrane with an exclusion size of 50 kD, HypC-form 3 was the only species found in the flowthrough (Figure 7, lane 8). Nevertheless, raising the concentration of this HypC species leads to oligomerization again (data not shown).

In Vitro Complex Formation between Pre-HycE and HypC in Extracts. To test whether HypC could exert its pre-HycE-binding activity also in vitro, the purified, native protein was incubated with S-100 extracts of strains HD705 (Δ*hycE*, Figure 8A, lane 3) and DHP-C (Δ*hypC*, Figure 8A, lane 4), respectively, for 30 min at 30 °C. Samples were subjected to nondenaturing PAGE and the appearance of the pre-HycE-HypC complex was detected immunologically with α-HypC antiserum. While no complex is formed in the Δ*hycE* strain (Figure 8A, lane 3), the purified HypC protein can bind to pre-HycE in the extract from strain DHP-C, generating HypC-form 1 (Figure 8A, lane 4). Surplus HypC that does not bind to pre-HycE migrates as a smear and in HypC-form 3 but is not competent to induce HypC-form 2.

In Vitro Complex Formation between Pre-HycE and HypC with Purified Components. Up to now it was impossible to preclude that also other components participate in the build-up of the pre-HycE-HypC complex. To exclude this possibility it seemed reasonable to try to reconstitute the complex with purified components. Therefore, *Strep-tag II* pre-HycE (*nik*) (Figure 8B, lane 3) was incubated with native HypC (Figure 8B, lane 4) for 30 min at 30 °C. The sample was then subjected to nondenaturing PAGE, and the appearance of the complex was detected by immunoblotting analysis using α-HypC antiserum. As shown in Figure 8C (lane 3), the complex is indeed reconstituted by mixing its two components, pre-HycE and HypC, whereas no such band is visible when the same amount of HypC is incubated in the absence of *Strep-tag II* pre-HycE (*nik*) (Figure 8C, lane 4). Due to the *Strep-tag II* peptide at the N-terminus of pre-HycE, the complex migrates slightly slower than its equivalent in strain HD709 (Figure 8C, lane 2).

DISCUSSION

Assembly of the metal containing active site of [NiFe] hydrogenases requires the function of a number of accessory proteins. For *E. coli* hydrogenase 3, six proteins (HypA, HypB, HypC, HypD, HypE, and HypF) were shown to be involved in this process (*7*, *9*−*11*). Their specific function

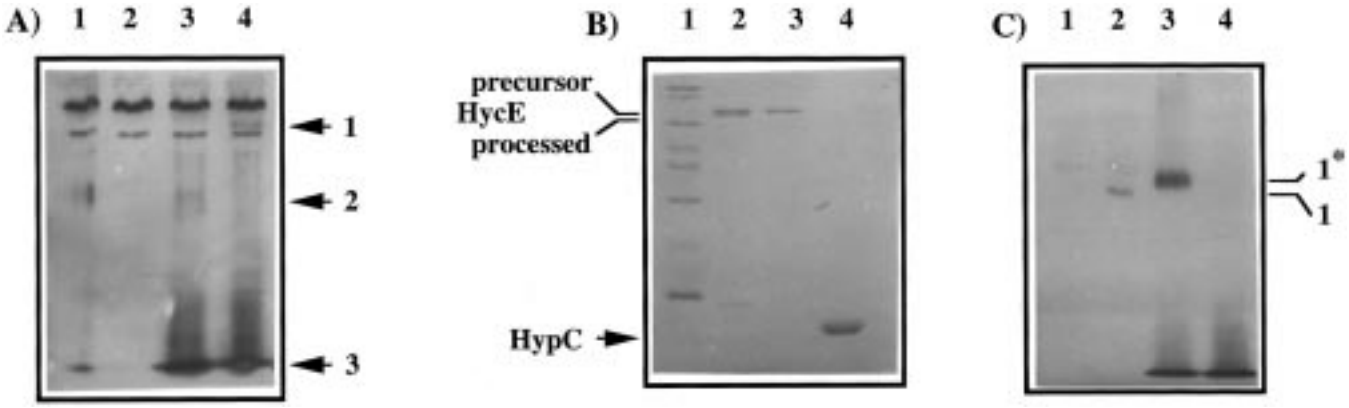

FIGURE 8: Complex formation between HycE and HypC in vitro. A: Generation of the complex in extracts. Chemoluminogram of extracts from strain HD705 (lane 1 and 3) or DHP-C (lane 2 and 4). Samples were incubated in the absence (lane 1 and 2) or presence (lane 3 and 4) of purified HypC protein. After nondenaturing PAGE, the HypC-form 1 was detected with α-HypC antiserum and is marked with an arrow. B: *Strep-tag II*-pre-HycE (*nik*) (lane 3, 1 μg) and native HypC (lane 4, 5 μg) used for in vitro complex formation experiments were subjected to 15% SDS-PAGE and stained with Coomassie blue. Lane 1: marker proteins (97 kD, 85 kD, 55 kD, 39 kD, 33 kD, 27 kD, 19 kD, 14 kD); lane 2: HycE, precursor and processed form (1 μg). C: Chemoluminogram. Generation of the complex with purified components. Either 0.85 μg HypC alone (lane 4) or 0.85 μg HypC plus 0.85 μg*Strep-tag II*-pre-HycE (*nik*) (lane 3) were incubated for 30 min at 30 °C. After 10% nondenaturing PAGE, the pre-HycE-HypC complex was detected using α-HypC antiserum. Lanes 1 and 2: S-100 extracts of strains DHP-C and HD709, respectively. The HypC-form 1 of strain HD709 is marked by "1", while the in vitro generated HypC-form 1 is marked by "1*".

and reaction sequence, however, is unknown up to know. It is open whether the *hyp* gene products act on HycE singly or in a concerted action as some kind of "Ni-incorporation complex" (*25*). Experimental evidence for the existence of a complex between HycE and one of the Hyp proteins, however, could not be provided yet.

With the aid of specific antibodies against most of the *E. coli* Hyp proteins and the establishment of a nondenaturing gel electrophoresis system with immunological detection, it was possible to look for putative interactions between Hyc and Hyp components. The in vitro processing reaction set up previously (*7*) was used to correlate possible changes of the migration behavior of HycE with the processing reaction. It was indeed possible to demonstrate the generation of a new HycE form which corresponds well with the predominant HycE form found in the wild-type (Figure 1). Upon processing, the calculated molecular weight of HycE changes by 3.85 kD and the net charge of the protein is increased from −14.8 to −20.6 at pH 8.8. Nevertheless, the rather dramatic change in migration behavior observed certainly is also due to a conformational change that traps the active site within the protein, as also proposed for the *D. gigas* enzyme (*2*). A severe problem though is the unusual migration behavior of pre-HycE in nondenaturing PAGE. In all strains tested but the wild-type, pre-HycE migrates as a smear of multiple conformers, which could consist of folding intermediates (possibly aberant folding states) or could be due to a high conformational flexibility of the HycE precursor protein due to the presence of the unprocessed C-terminus which is supposed to keep the protein in an "open" conformation competent for metal incorporation (2, 26). Therefore at present we cannot explain what it means that only 30% of the pre-HycE antigen is being processed while about 50% of it is converted into the new, fast migrating HycE species (Figure 1).

Since the chosen gel system seemed nevertheless suitable, we looked for a change in migration behavior of various Hyp proteins in different strains which carry mutations in genes required for hydrogenase activity. Such a change could only be observed in the case of HypC. The migration behavior of HypB, HypD, HypE, and HypF is not affected by any of the tested mutations and no higher molecular weight complexes could be observed, which does not support the idea of a "metal-incorporation complex". However, this possibility can certainly not be excluded completely, as weak interactions would probably have been undetectable with this method.

It was striking that in nondenaturing PAGE, the 9.7 kD protein HypC migrates in at least three forms, which exhibit remarkably different migration behavior (Figure 2). The appearance of one of these forms (form 1) was dependent on the presence of HycE precursor in the extract. The trace of HypC-form 1 in wild-type extracts is probably due to the about 5% unprocessed HycE present in these cells grown under these conditions. HypC-form 3 seems to be the free, probably dimeric form of HypC, as its elution behavior during anion exchange chromatography (Mono-Q) corresponds well to the elution behavior of overproduced, native HypC from a Mono-Q column during purification. The slight difference in the elution behavior could be due to the different salts used for the elution in the two experiments. The identity of HypC-form 2 is yet unknown. Its absence in S-100 extracts of strains DHP-B and DHP-D implies that this form could consist of a complex between HypC, HypB, and HypD. Although we do not have any evidences that support this idea (the migration behaviors of HypB and HypD in nondenaturing PAGE and during anion exchange chromatography are indifferent to the presence or absence of HypC in the extract), we cannot rule out this possibility completely if e.g. immunoblotting analysis is too insensitive to detect HypB or HypD in HypC-form 2. Taking into account the migration behavior of purified HypC in nondenaturing PAGE, yet another possible identity of HypC-form 2 could be a certain oligomeric state of HypC.

The results presented above suggest that HypC-form 1 could represent a complex between the HycE precursor and HypC. This notion is strengthened by experiments, in which each one of the potential interacting partners was overproduced and the influence of the overproduction on occurrence and amount of HypC-form 1 was investigated (Figure 3). The data show (i) that the HypC-form 1 cannot be generated in the absence of pre-HycE, not even by overproduction of HypC, and (ii) that the overexpression of *hycE* results in an increase or a generation of HypC-form 1 at the expense of HypC-form 2 (Figure 3B). Therefore, overproduced pre-HycE seems to bind preferentially to HypC-form 2 to generate HypC-form 1. However, it cannot be excluded that overexpression of *hycE* prevents a conversion of HypC-form 1 into HypC-form 2.

Since comigration experiments in the one-dimensional nondenaturing gel system could not be performed due to the undefined migration of pre-HycE, we used two-dimensional gel electrophoresis (Figure 4) and anion exchange chromatography (Figure 5) to clearly demonstrate comigration and a physical interaction between pre-HycE and HypC. Obviously (Figure 4), only a certain conformer of pre-HycE is competent to bind HypC stably, while the majority of the pre-HycE antigen cannot participate in this interaction. Currently we do not know what distinguishes HypC-binding-competent pre-HycE from pre-HycE that is not competent of binding. Another possibility would be that the amount of HypC in the cell is less than stoichiometric relative to the amount of pre-HycE and is recycled after its release from the large subunit, as proposed for the NarJ protein (28 and G. Giordano, personal communication).

Interestingly, the pre-HycE-HypC protein complex can also be generated in vitro in extracts (Figure 8A) as well as with purified components (Figure 8C). Incubation of purified HypC with an S-100 extract of strain DHP-C (Δ*hypC*) leads to the formation of a small but significant amount of HypC-form 1 (Figure 8A). Again, formation of this HypC form is specific and strictly dependent on the presence of pre-HycE and cannot be observed in strain HD705 (Δ*hycE*). This experimental setup resembles the in vitro Ni-incorporation system established in our laboratory (*7*). In strain DHP-C, HycE accumulates in the Ni-free precursor form (*9*) and upon addition of HypC, all components required for metal-incorporation and C-terminal processing are present in the extract. Nevertheless, no processing of pre-HycE takes place (data not shown), even though purified HypC is active in the sense that it can exert its pre-HycE-binding function (Figure 8A and 8C). It seems that pre-HycE does not remain in an activatable state in the Δ*hypC* mutant, like it is the case in strain NCI900 (*nikA*$^-$, ΔhycI). Possible explanations

for this phenomenon could be that (i) in the absence of HypC, other accessory Hyp proteins cannot act on pre-HycE in vivo, or that (ii) HypC is required to prevent misfolding of pre-HycE or to keep it in a certain conformation necessary for metal-incorporation. Generation of the pre-HycE-HypC complex by mixing its two purified components (Figure 8B and 8C) makes it highly unlikely that (i) HypC-form 1 contains other components than pre-HycE and HypC and (ii) that the generation of the complex requires the help of other proteins.

hypC has a homologous gene in the operon coding for hydrogenase 2, namely *hybG* (*27*). Mutations in *hybG* abolish the maturation of the large subunit from hydrogenase 1 and 2 (27), but not of hydrogenase 3. It is plausible to assume that HybG interacts with the precursor of the large subunits of hydrogenases 1 and 2 in the same manner as demonstrated for HypC in the maturation of hydrogenases 3.

In summary, the data presented suggest that HypC could be a hydrogenase specific "chaperone-like" protein that binds to the precursor form of the large subunit of *E. coli* hydrogenase 3 and "guides" it through the posttranslational maturation process. As the pre-HycE-HypC complex is present in all other *hyp* mutants, binding seems to be an early step in maturation. Until now we do not know at what step in the processing scheme the dissociation occurs. The absence of bound Ni or Fe in the purified HypC protein does not support the idea that HypC is directly involved in metal-donation to pre-HycE. The stoichiometry between pre-HycE and HypC in the complex and the binding site between the two components are presently under investigation.

A similar function has been proposed recently for the NarJ protein. Liu et al. (*28*) propose NarJ to be a system-specific chaperone required for biogenesis of an active respiratory nitrate reductase complex (encoded by *narG*, *narH*, and *narI*) in *E. coli*. Furthermore it was shown that binding of NarJ to the molybdenum cofactor containing catalytic subunit, NarG, is required for the insertion of the cofactor into the apo-NarG subunit (G. Giordano, personal communication).

Binding of accessory proteins to a Ni-free apoprotein was also demonstated recently for *Klebsiella aerogenes* urease. Three accessory proteins, UreD, UreF, and UreG, form a complex with the urease apoprotein, and this is thought to be the key activation complex in the cell (*29*). Therefore, binding of accessory proteins as a prerequisite for active site assembly could be a common pattern in catalyzed metal incorporation.

ACKNOWLEDGMENT

We are grateful to G. Giordano for communication of results prior to publication. We want to thank Dr. Hartl of the Institut für Pharmazeutische Biologie der Universität München for performing AAS with HypC for us. Also we thank E. Zehelein for preparation of purified HycI protease and B. Neuhierl for critical reading of the manuscript.

REFERENCES

1. Peck, H. D., and Gest, H. (1957) *J. Bacteriol. 73*, 706−721.
2. Volbeda, A., Charon, M.-H., Piras, C., Hatchikian, E. C., Frey, M., and Fontecilla-Camps, J. C. (1995) *Nature 373*, 580−587.
3. Happe, R. P., Roseboom, W., Bagley, K. A., Pierik, A. J., and Albracht, S. P. J. (1997) *Nature 385*, 126.
4. Maier, T., and Böck, A. (1996b) in *Advances in Inorganic Biochemistry: Mechanisms of Metallocenter Assembly* (Hausinger, R. P., Eichhorn, G. L., and Marzilli, L. G., Eds.) pp 173−192, VCH Publishers: New York.
5. Rossmann, R., Sauter, M., Lottspeich, F., and Böck, A. (1994) *Eur. J. Biochem. 220*, 377−384.
6. Rossmann, R., Maier, T., Lottspeich, F., and Böck, A. (1995) *Eur. J. Biochem. 227*, 545−550.
7. Maier, T., and Böck, A. (1996a) *Biochemistry 35*, 10089−10093.
8. Menon, A. L., and Robson, R. L. (1994) *J. Bacteriol. 176*, 291−295.
9. Jacobi, A., Rossmann, R., and Böck, A. (1992) *Arch. Microbiol. 158*, 444−451.
10. Maier, T., Jacobi, A., Sauter, M., and Böck, A. (1993) *J. Bacteriol. 175*, 630−635.
11. Maier, T., Binder, U., and Böck, A. (1996) *Arch. Microbiol. 165*, 333−341.
12. Waugh, R., and Boxer, D. H. (1986) *Biochimie 68*, 157−166.
13. Maier, T., Lottspeich, F., and Böck, A. (1995) *Eur. J. Biochem. 230*, 133−138.
14. Olson, J. W., Fu, C., and Maier, R. J. (1997) *Mol. Microbiol. 24*, 119−128.
15. Begg, Y. A., Whyte, J. N., and Haddock, B. A. (1977) *FEMS Microbiol. Lett. 2*, 47−50.
16. Navarro, C., Wu, L.-F., and Mandrand-Berthelot, M.-A. (1993) *Mol. Microbiol. 9*, 1181−1191.
17. Laemmli, U. K. (1970) *Nature 227*, 680−685.
18. Tabor, S., and Richardson, C. C. (1985) *Proc. Natl. Acad. Sci. U.S.A. 82*, 1074−1078.
19. Studier, F. W., and Moffatt, B. A. (1986) *J. Mol. Biol. 189*, 113−130.
20. Miller, J. H. (1972) *Experiments in molecular genetics*, Cold Spring Harbour Laboratory, Cold Spring Harbour, N. Y.
21. Whitaker, J. R., and Granum, P. E. (1980) *Anal. Biochem. 109*, 156−159.
22. Voss, S., and Skerra, A. (1997) *Protein Engineering 10*, 975−982.
23. Maier, T., Drapal, N., Thanbichler, M., and Böck, A. (1997) *Manuscript in preparation*.
24. Wu, L.-F., and Mandrand-Berthelot, M.-A. (1986) *Biochimie 68*, 167−179.
25. Jacobi, A. (1994), Ludwig-Maximilians-Universität München.
26. Binder, U., Maier, T., and Böck, A. (1996) *Arch. Microbiol. 165*, 69−72.
27. Menon, N. K., Chatelus, C. Y., DerVartanian, M., Wendt, J. C., Shanmugam, K. T., Peck, H. D., and Przybyla, A. E. (1994) *J. Bacteriol. 176*, 4416−4423.
28. Liu, X., and DeMoss, J. A. (1997) *J. Biol. Chem. 272*, 24266−24271.
29. Moncrief, M. B. C., and Hausinger, R. P. (1997) *J. Bacteriol. 179*, 4081−4086.
30. Yanisch-Perron, C., Vieira, J., and Messing, J. (1985) *Gene 33*, 103−109.
31. Casadaban, M. J., and Cohen, S. N. (1979) *Proc. Natl. Acad. Sci. U.S.A. 76*, 4530−4533.
32. Sauter, M., Böhm, R., and Böck, A. (1992) *Mol. Microbiol. 6*, 1523−1532.
33. Wu, L.-F., Mandrand-Berthelot, M.-A., Waugh, R., Edmonds, C. J., Holt, S. E., and Boxer, D. H. (1989) *Mol. Microbiol. 3*, 1709−1718.
34. Lutz, S., Jacobi, A., Schlensog, V., Böhm, R., Sawers, G., and Böck, A. (1991) *Mol. Microbiol. 5*, 123−135.

BI9720078